天 氣 學 二

(Synoptic Meteorology II)

上課時間: 10:20～12:10 Wednesday, B105

授課教師: 游政谷

email: yuku@ntu.edu.tw

Chapter 1 Extratropical Cyclones

1.6 Cloud and precipitation within EC

Houze (2014)

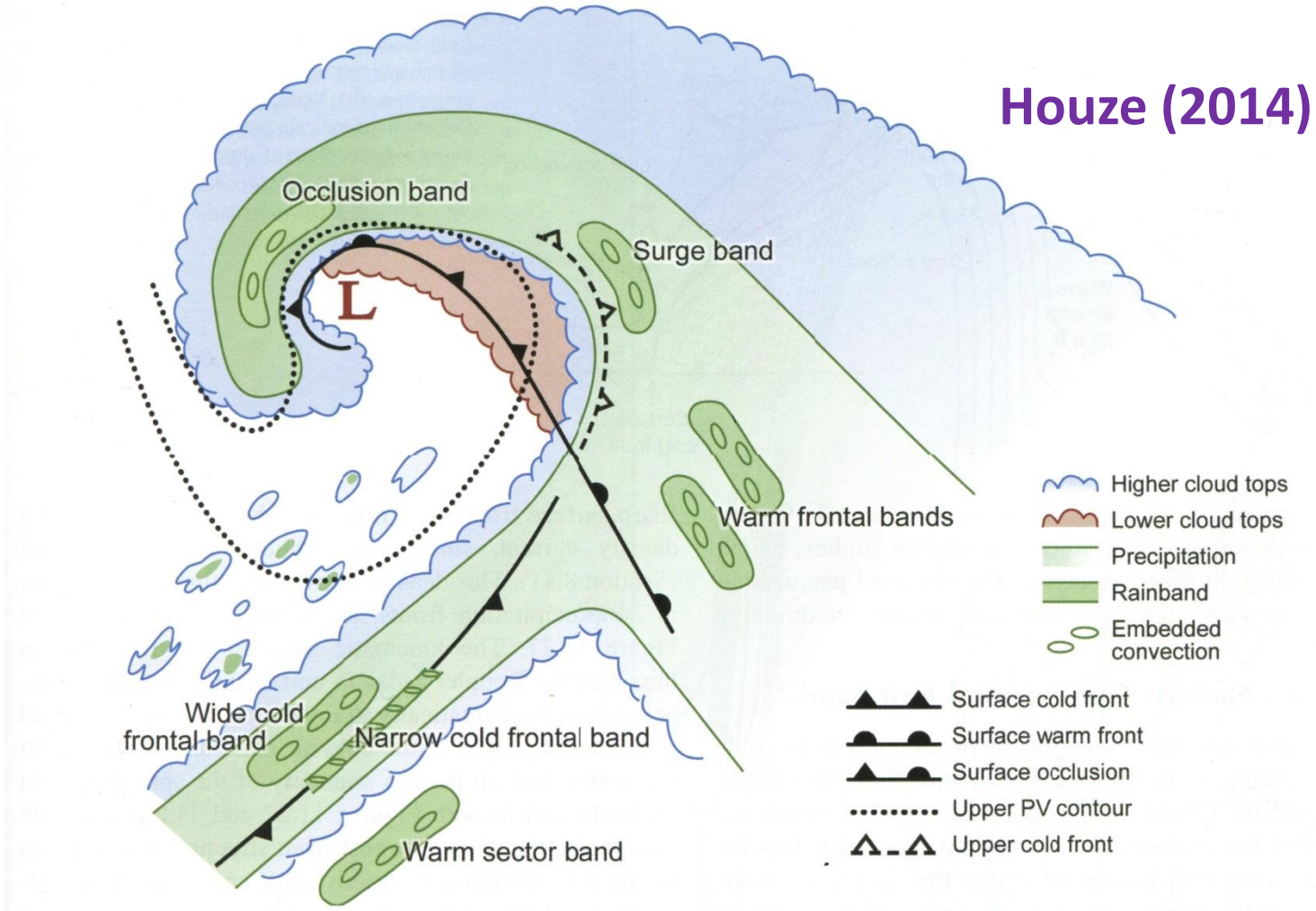

FIGURE 11.24 Idealization of the cloud and precipitation pattern associated with a mature extratropical cyclone.

隨著溫帶氣旋的通過, 垂直指向都卜勒雷達(vertically pointing Doppler radar)所量測的降水粒子的下降速度, 以及逐時雨量隨時間的變化(Houze et al. 1976)

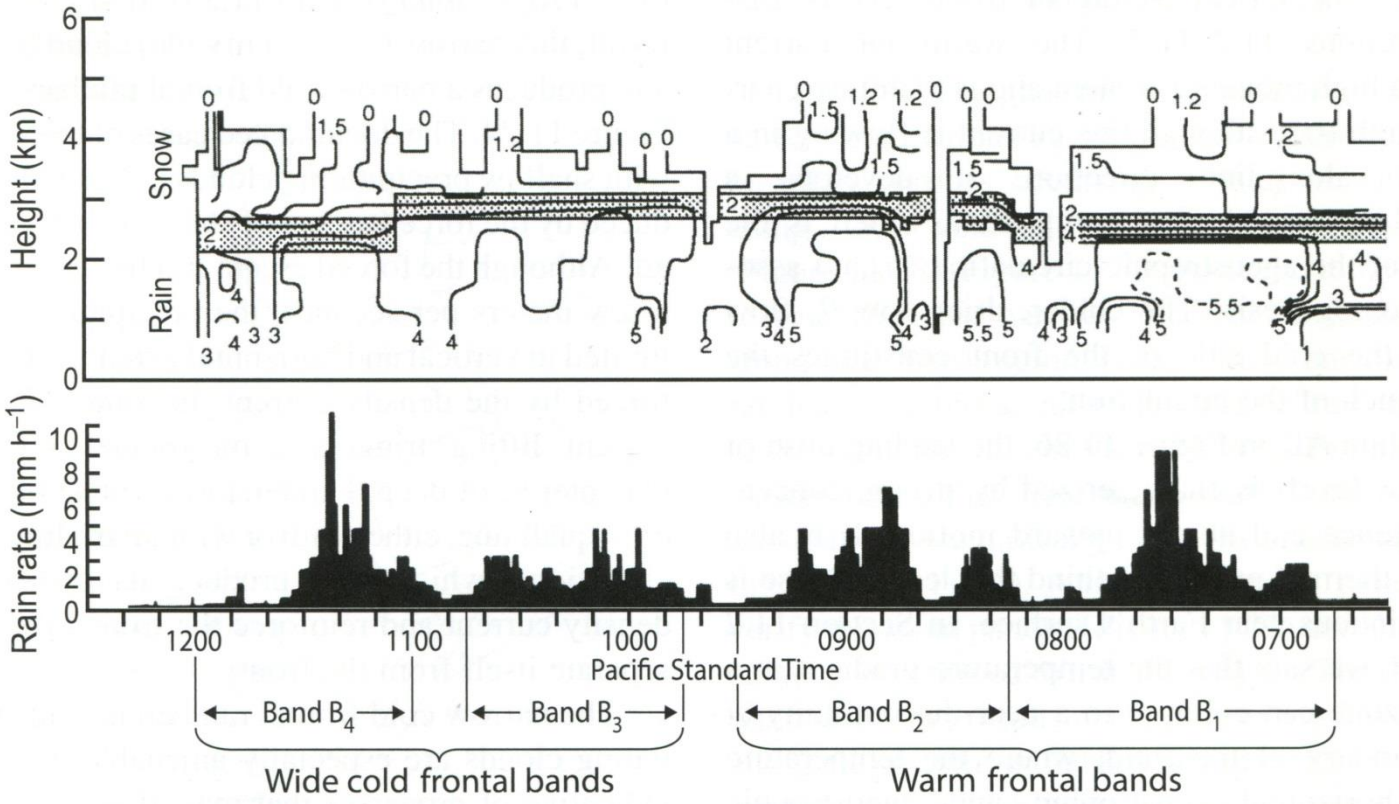

Time–height cross section of vertically pointing Doppler radar data and high resolution rain gauge trace obtained during the passage of an extratropical cyclonic storm over Seattle, Washington. Radar data show 10-min average precipitation fallspeeds (m s^{-1}). The melting layer, characterized by a large gradient of fallspeed, is shaded for emphasis. Contours labeled with zeros outline the region of precipitation detected by the radar. *Adapted from Houze et al. (1976). Republished with permission of the American Meteorological Society.*

Wide cold frontal rainbands (WCFR) are dominantly stratiform rain, are associated with a layer of enhanced mean ascent above the cold front, and generally move with embedded winds

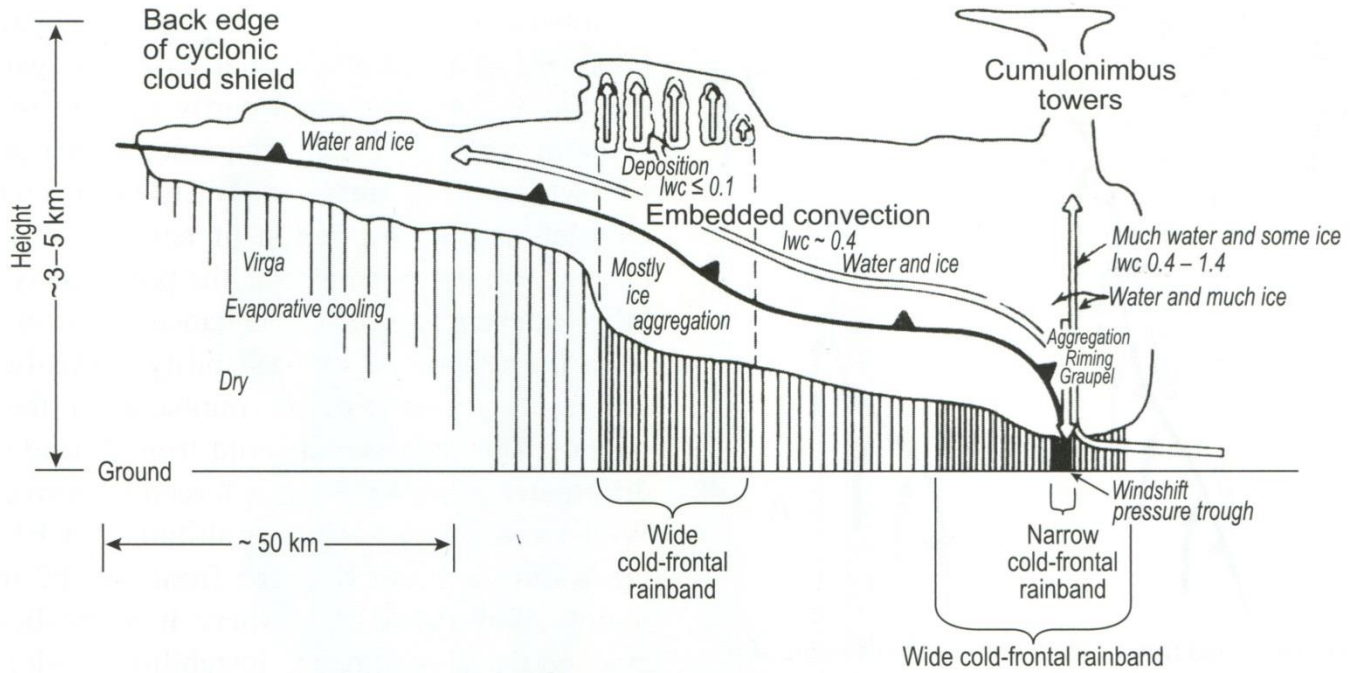

Cloud structure, air motion, and precipitation mechanisms at a cold front as revealed by instrumented aircraft, radar, and other observations of frontal cyclones passing over Washington State. Vertical hatching below cloud bases represents precipitation: the density of the hatching corresponds qualitatively to the precipitation rate. Open arrows depict airflow relative to the front: a strong convective updraft and downdraft above the surface front and pressure trough, and broader ascent over the cold front aloft. Cloud liquid water contents (lwc) are in g m^{-3}. The motion of the rainband is from left to right. Horizontal and vertical scales are approximate but typical of aircraft and radar observations in specific cases. *From Matejka et al. (1980). Republished with permission of the Royal Meteorological Society.*

窄冷鋒雨帶(NCFR)位於寬冷鋒雨帶(WCFR)內 (Yu and Smull 2000)

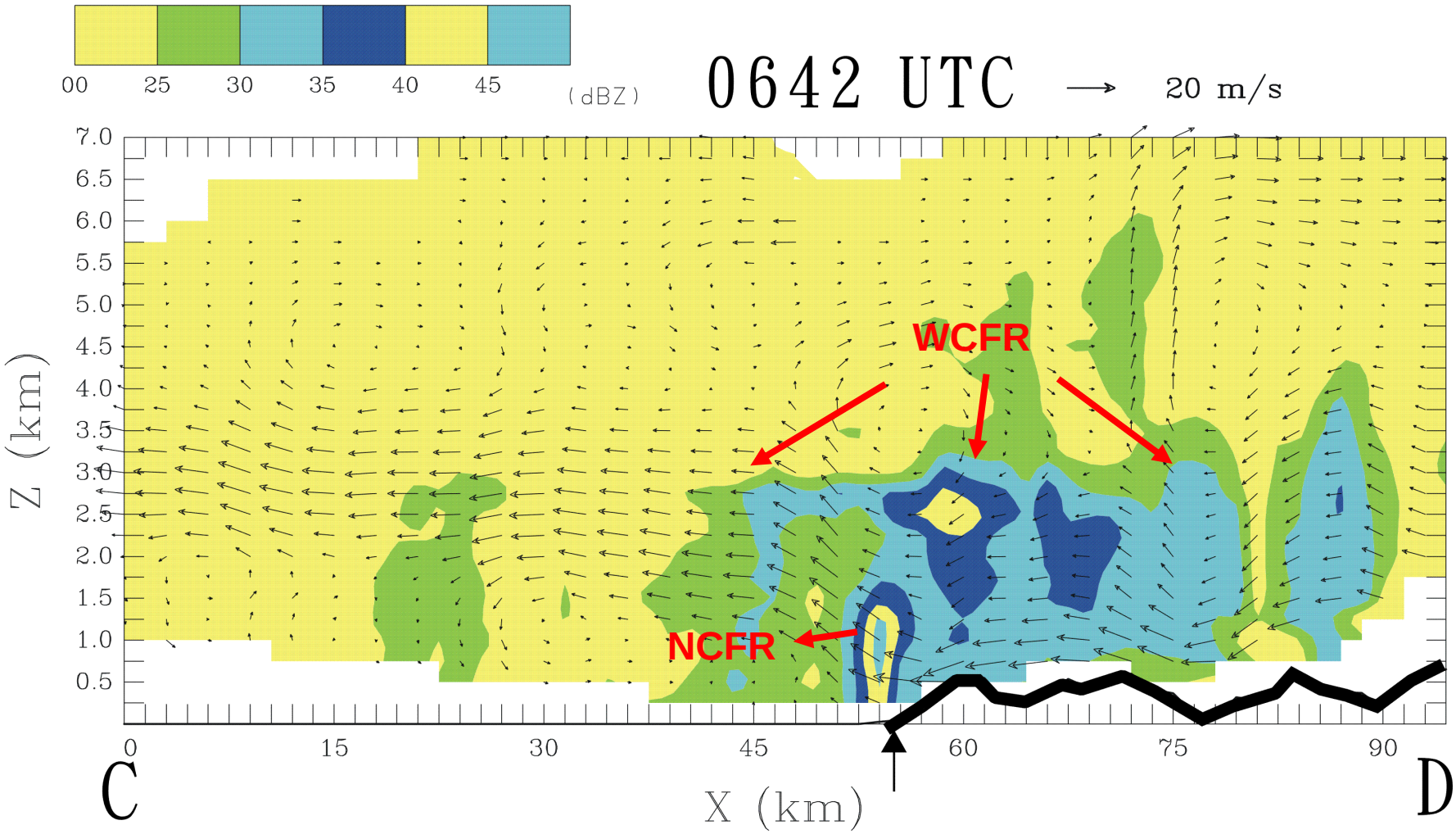

寬冷鋒雨帶移動速度比窄冷鋒雨帶快, 所以到最後趕上窄冷鋒雨帶並超越它
(Hobbs et al. 1980)

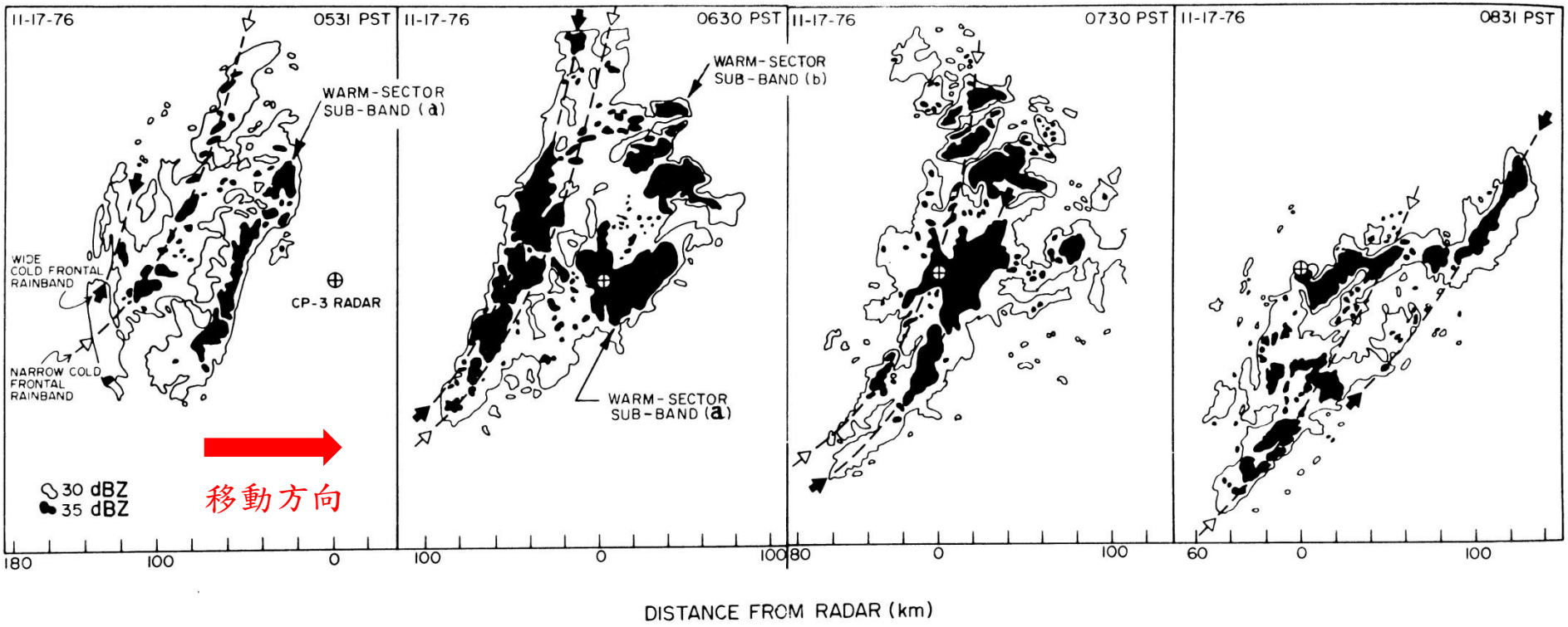

冷鋒面中小尺度結構
(Shapiro et al. 1985)

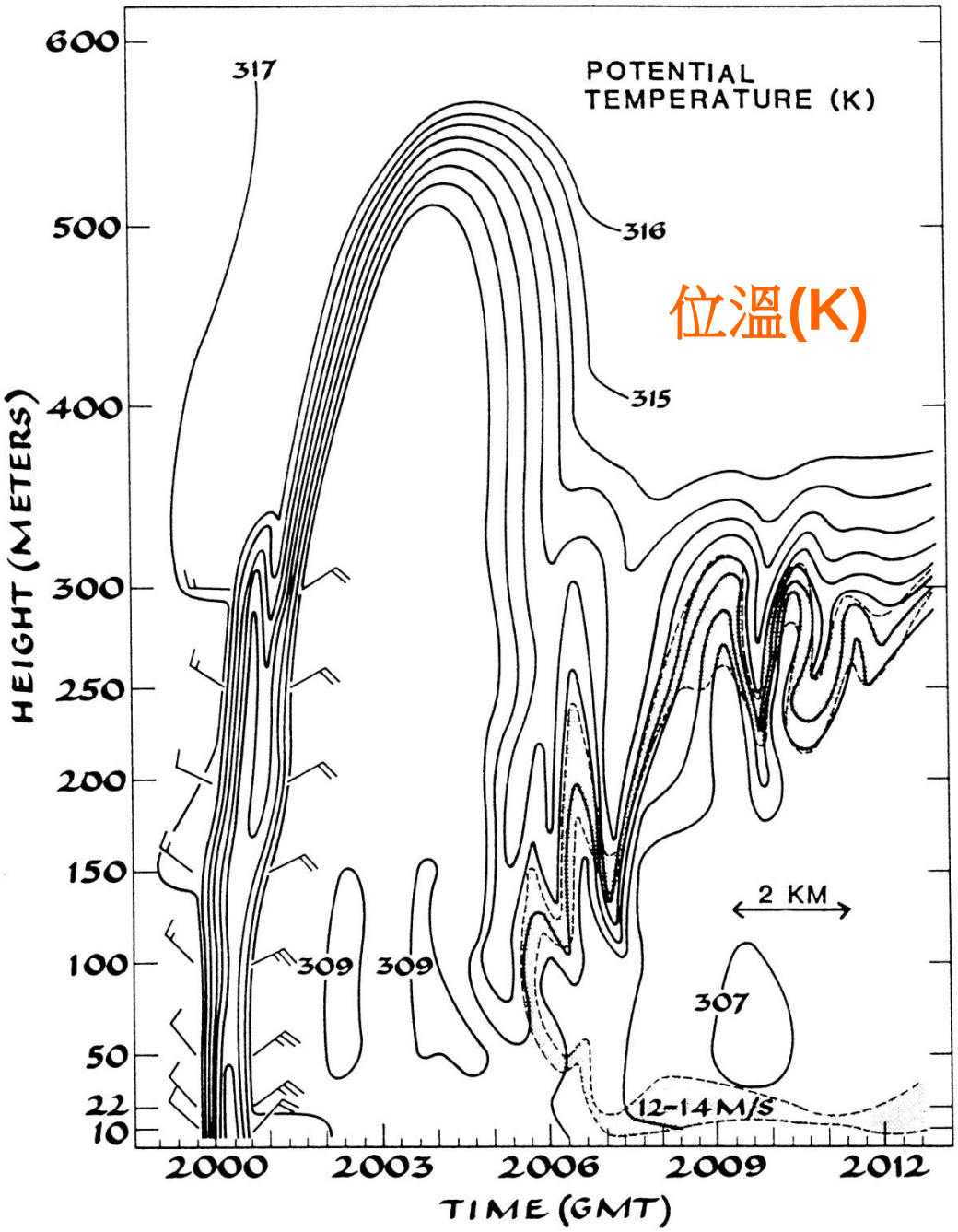

位溫(K)

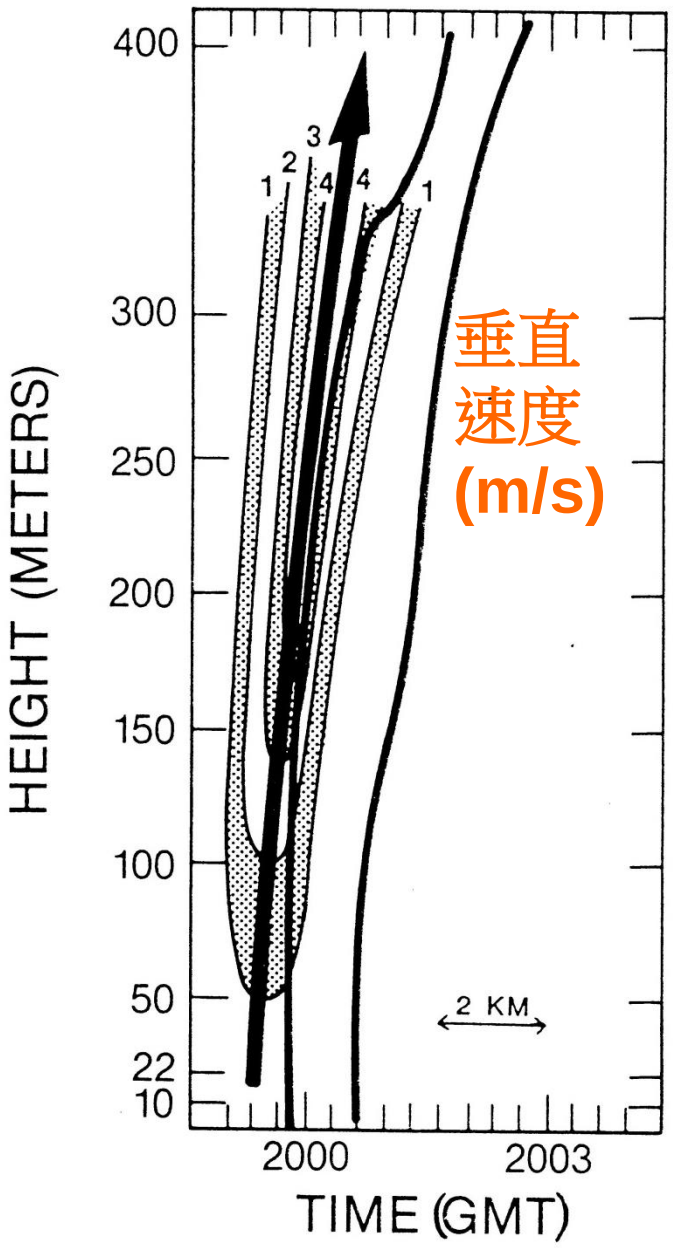

垂直速度
(m/s)

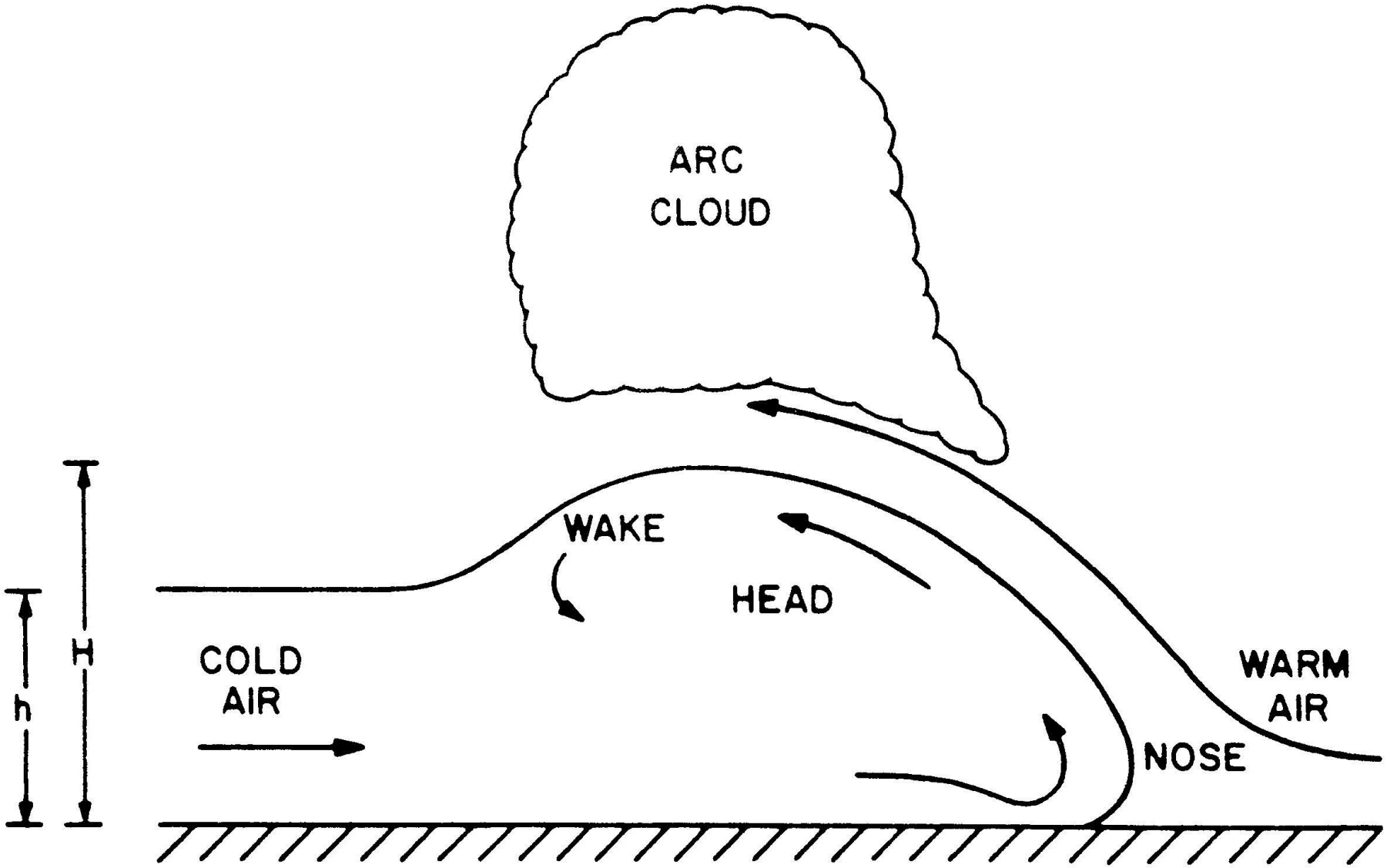

Schematic representation of an atmospheric density current. (After Goff, 1976)

Density current movie in the lab.

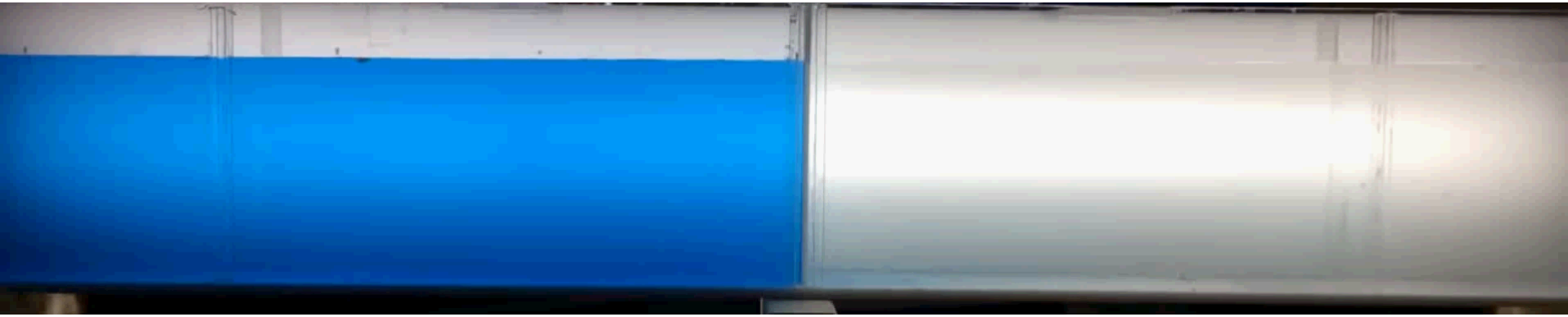

Precipitation-induced cold air feeding the leading edge of a surface front

Seitter and Muench 1985

Schematic representation of the hypothesized mechanism responsible for the 4 May 1983 rope cloud.

Visible satellite image showing an example of rope cloud (Seitter and Muench 1985)

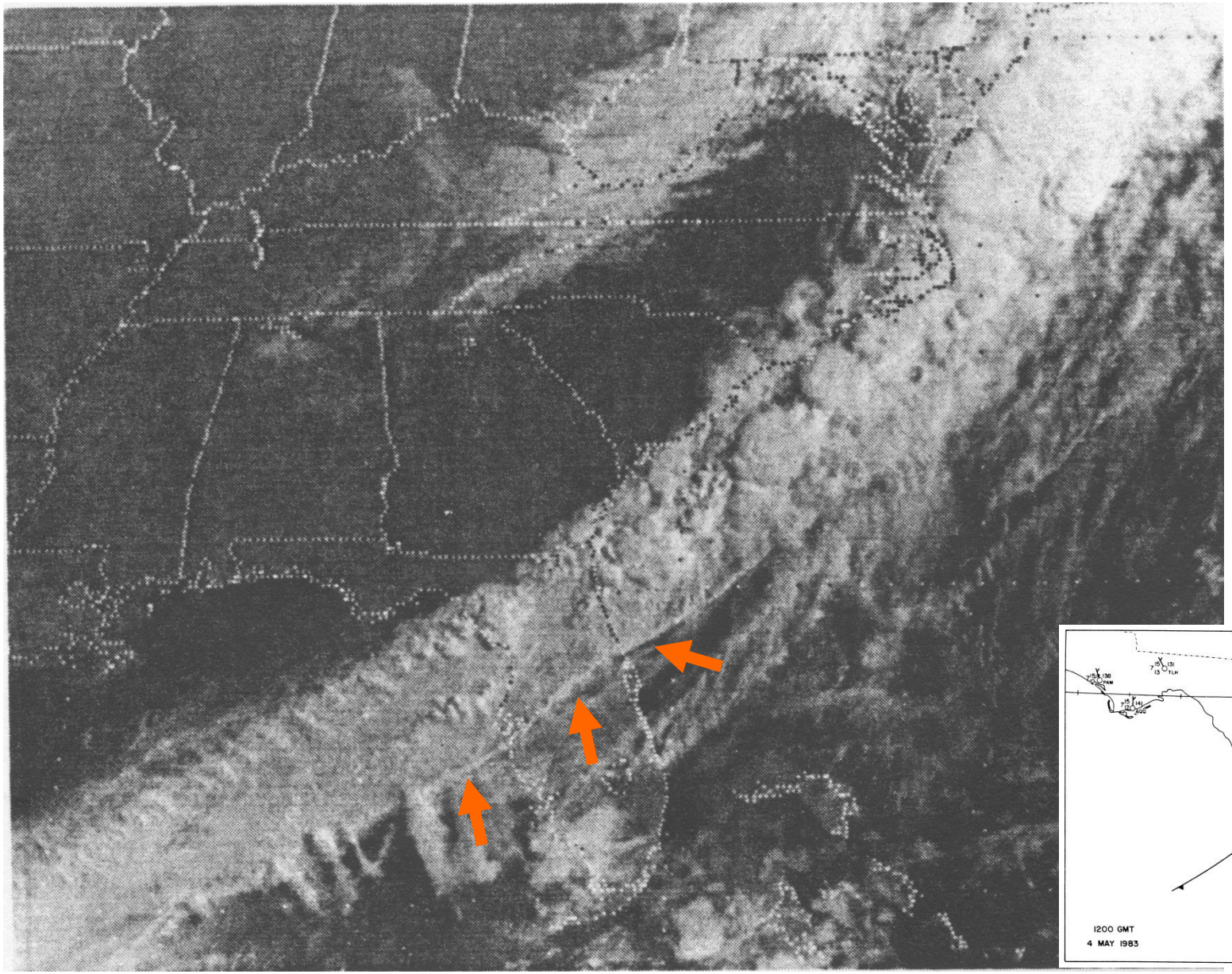

在中緯度窄冷鋒雨帶的鋒前環境可能具有對流穩定的大氣
(Yu and Smull 2000)

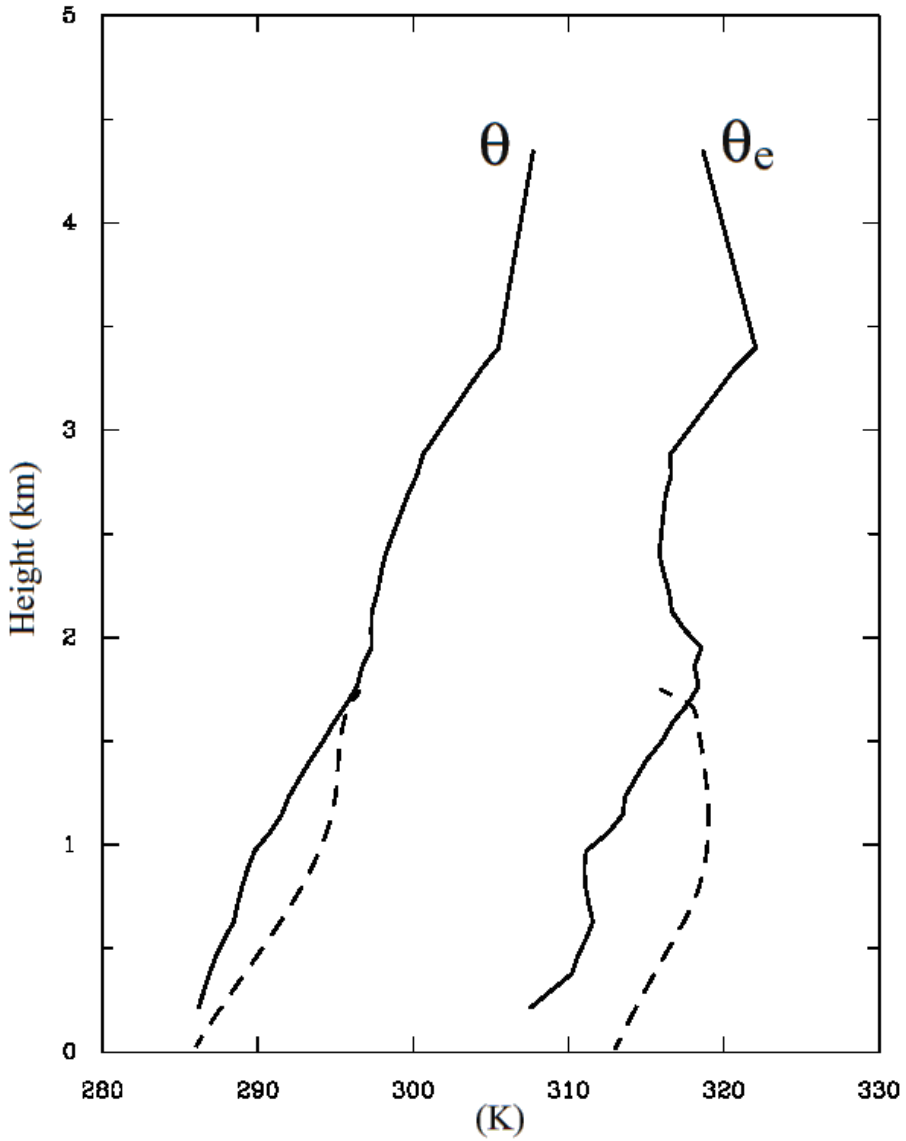

典型的熱帶探空, 中低對流層為對流不穩定的大氣 (Ooyama 1969)

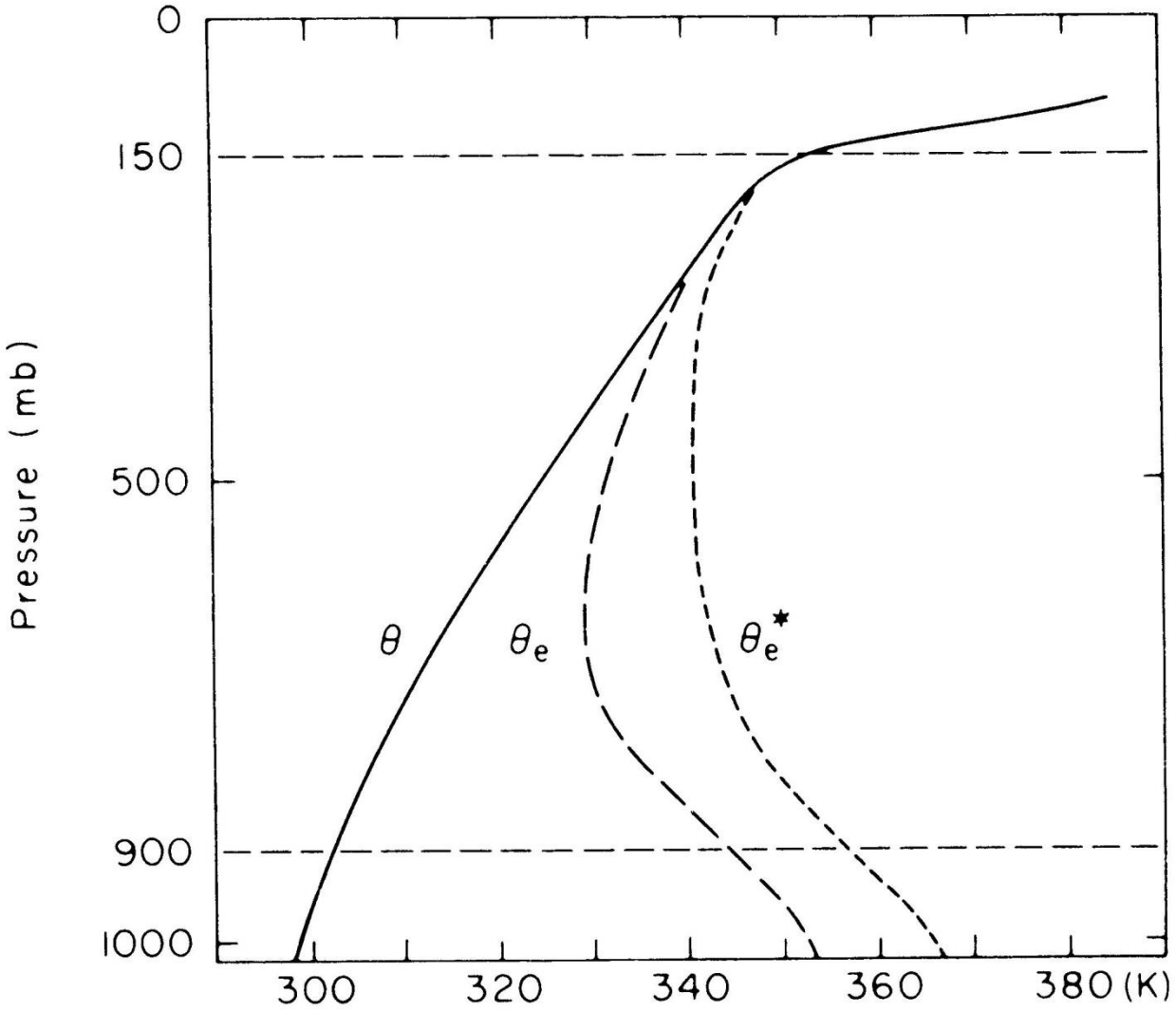

NCFR之回波與風場垂直結構, 中性大氣但可以產生極強降水回波 (Carbone 1982)

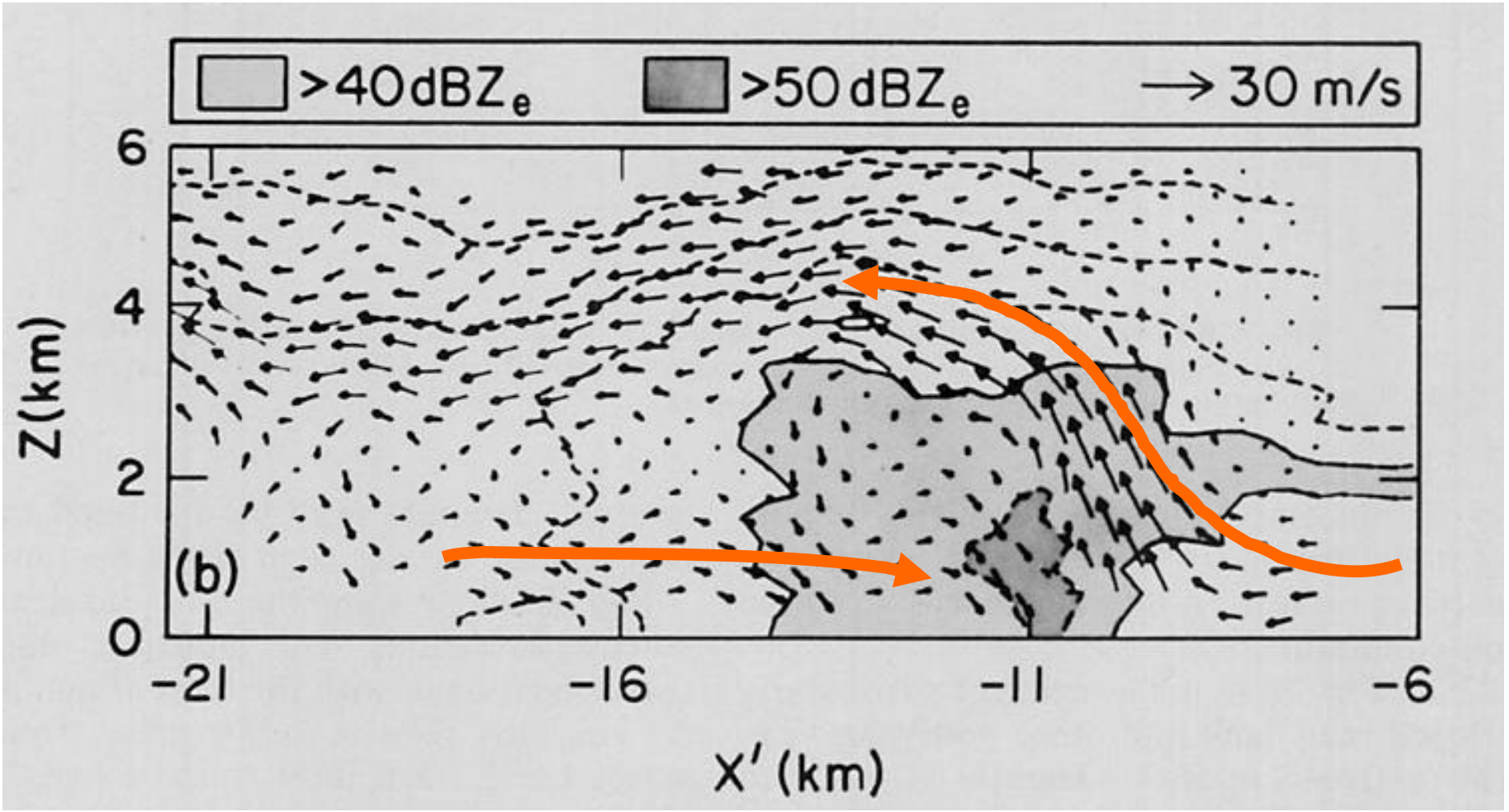

伴隨NCFR之雷達回波特徵 (Hobbs and Biswas 1979)

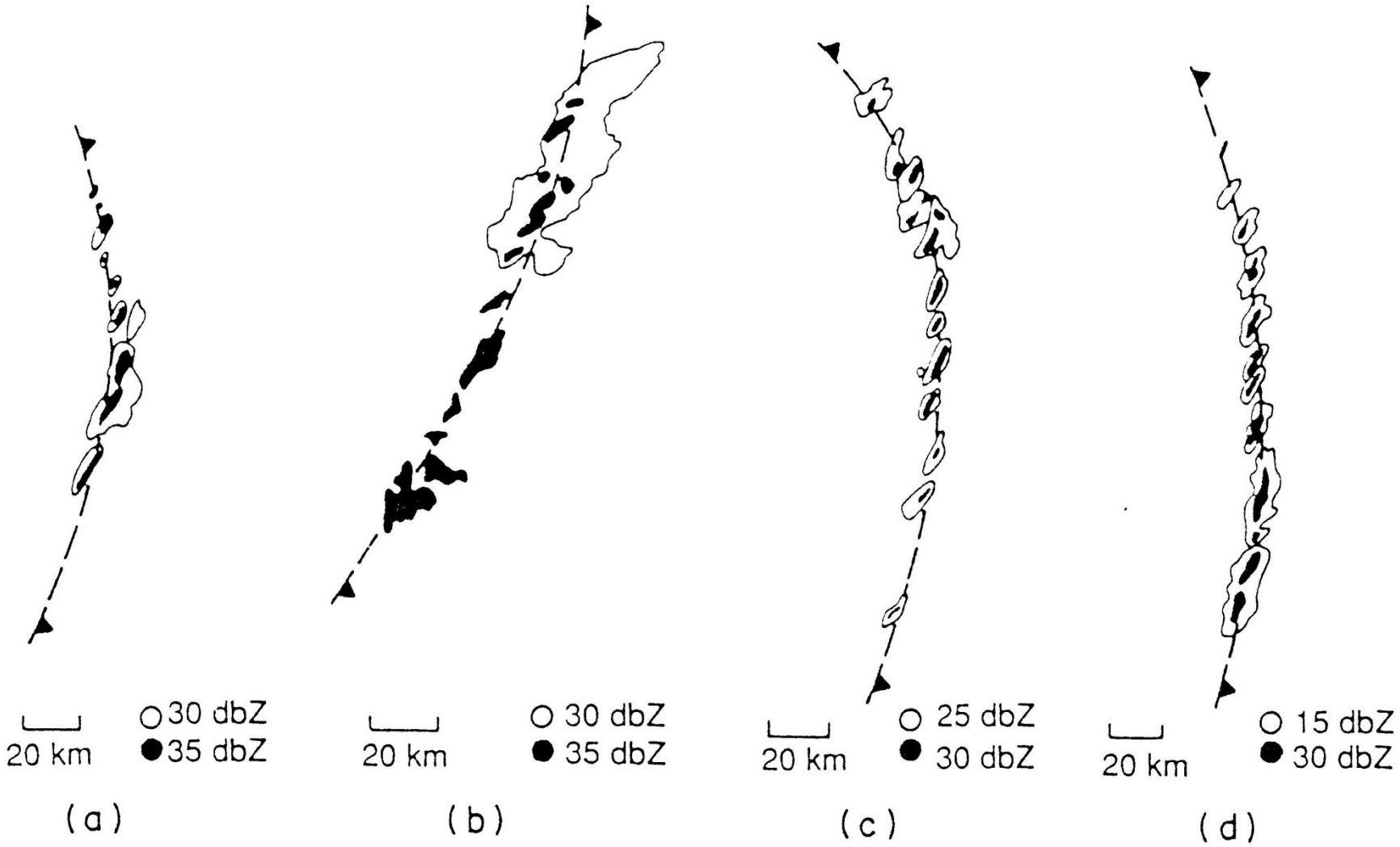

冷鋒風切線(wind shift line)發展出波動形式示意圖
(Hobbs and Persson 1982)

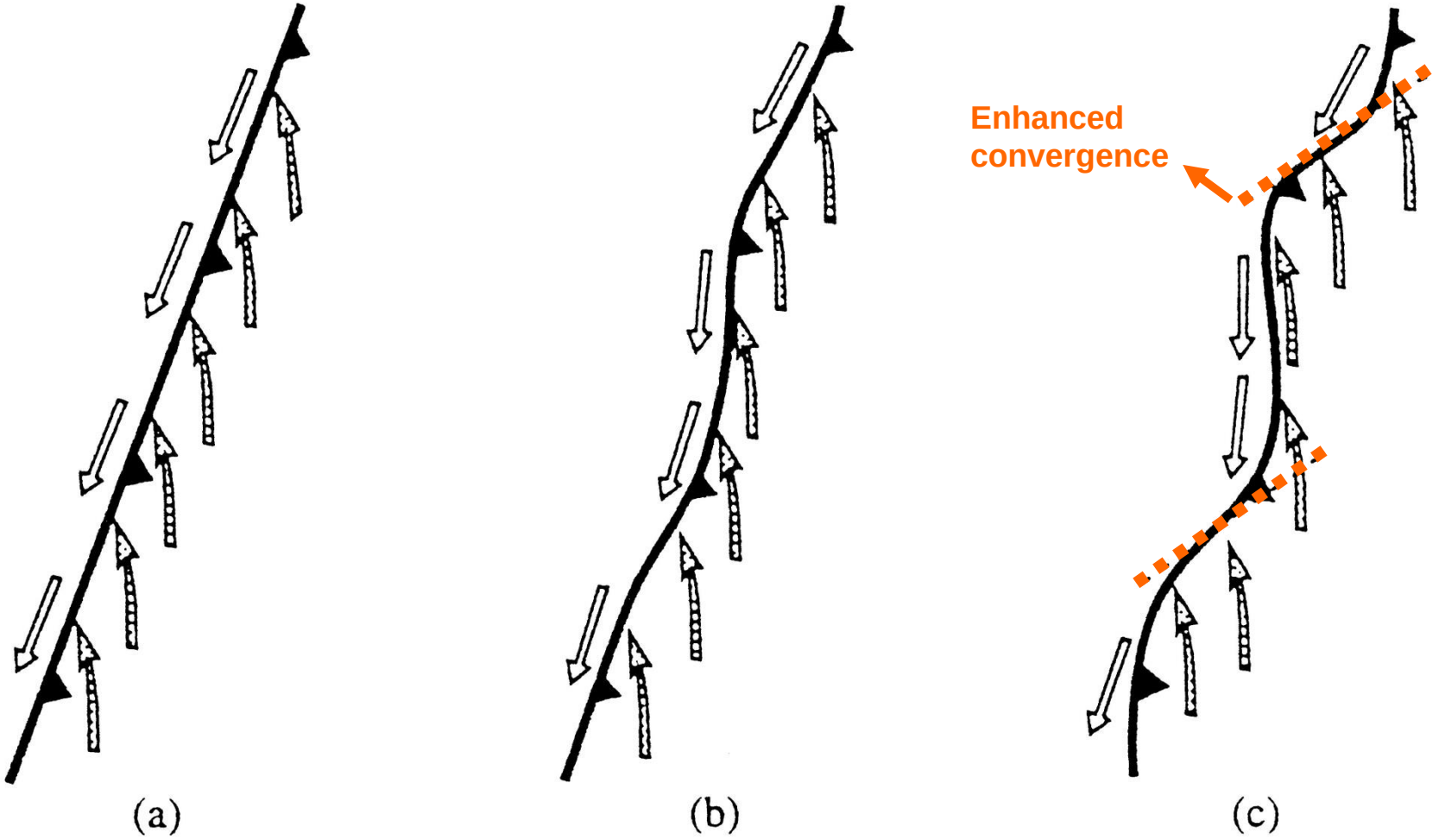

NCFR之降水中心(precipitation core)與缺口(gap region)與鋒面風切帶相關位置示意圖 (Hobbs and Persson 1982)

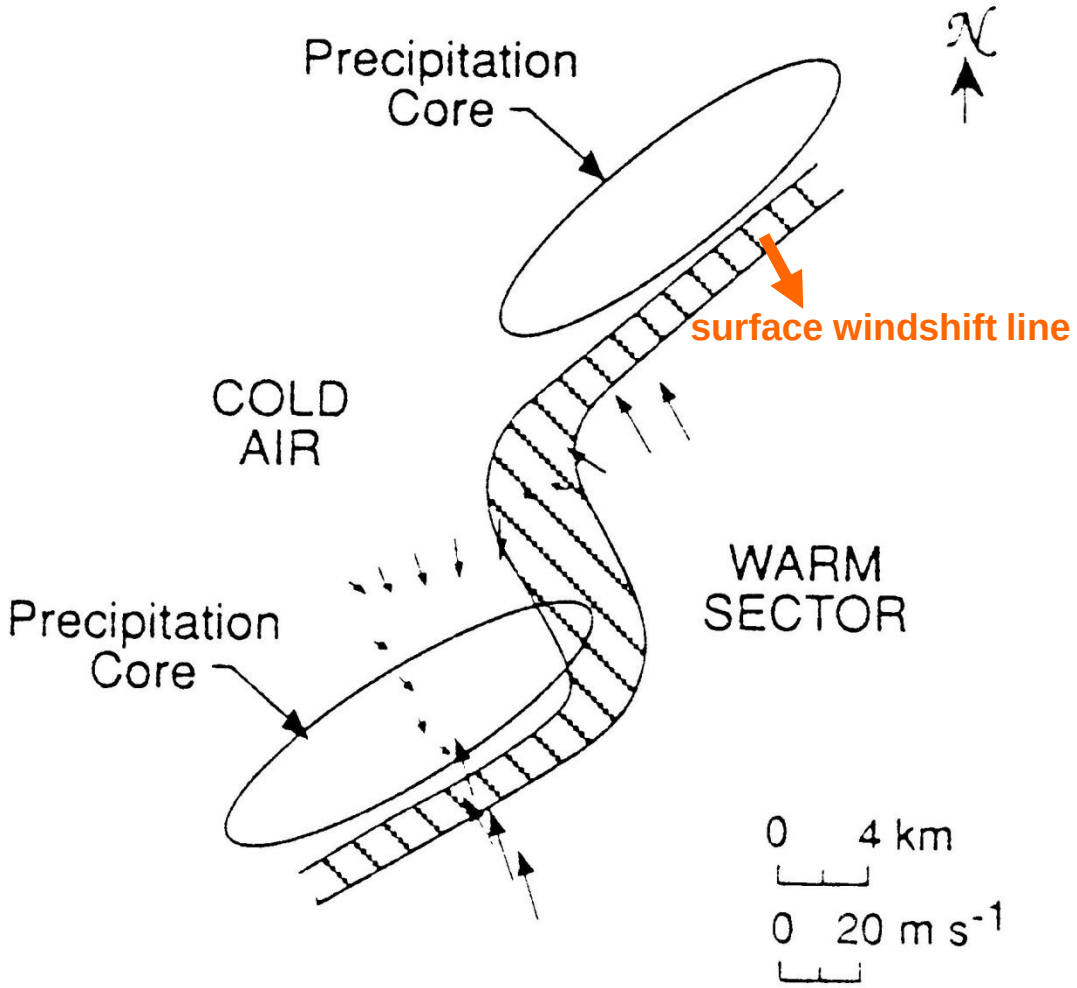

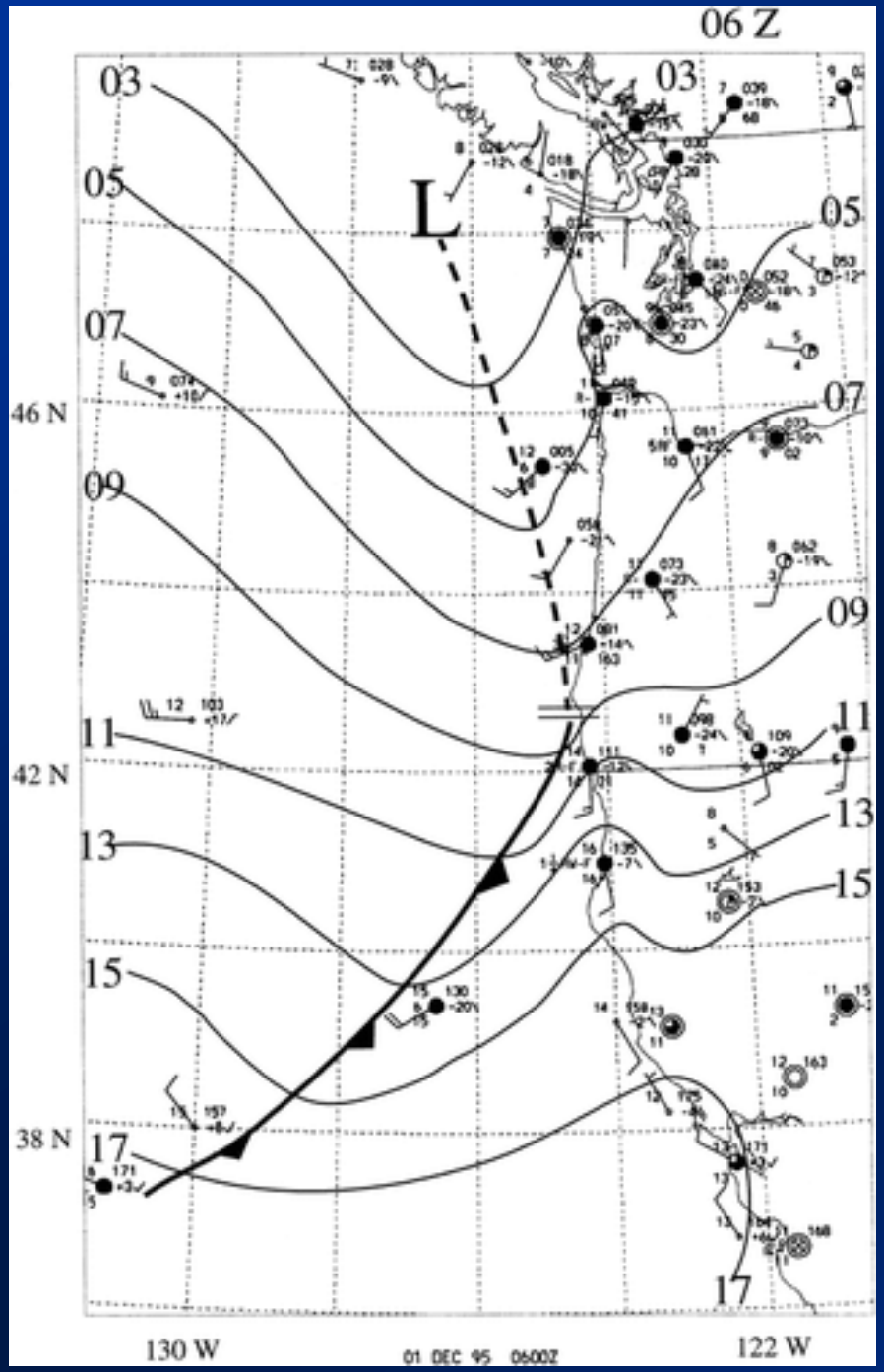

Surface analysis at 06 UTC
1 Dec. 1995
(Yu and Smull 2000)

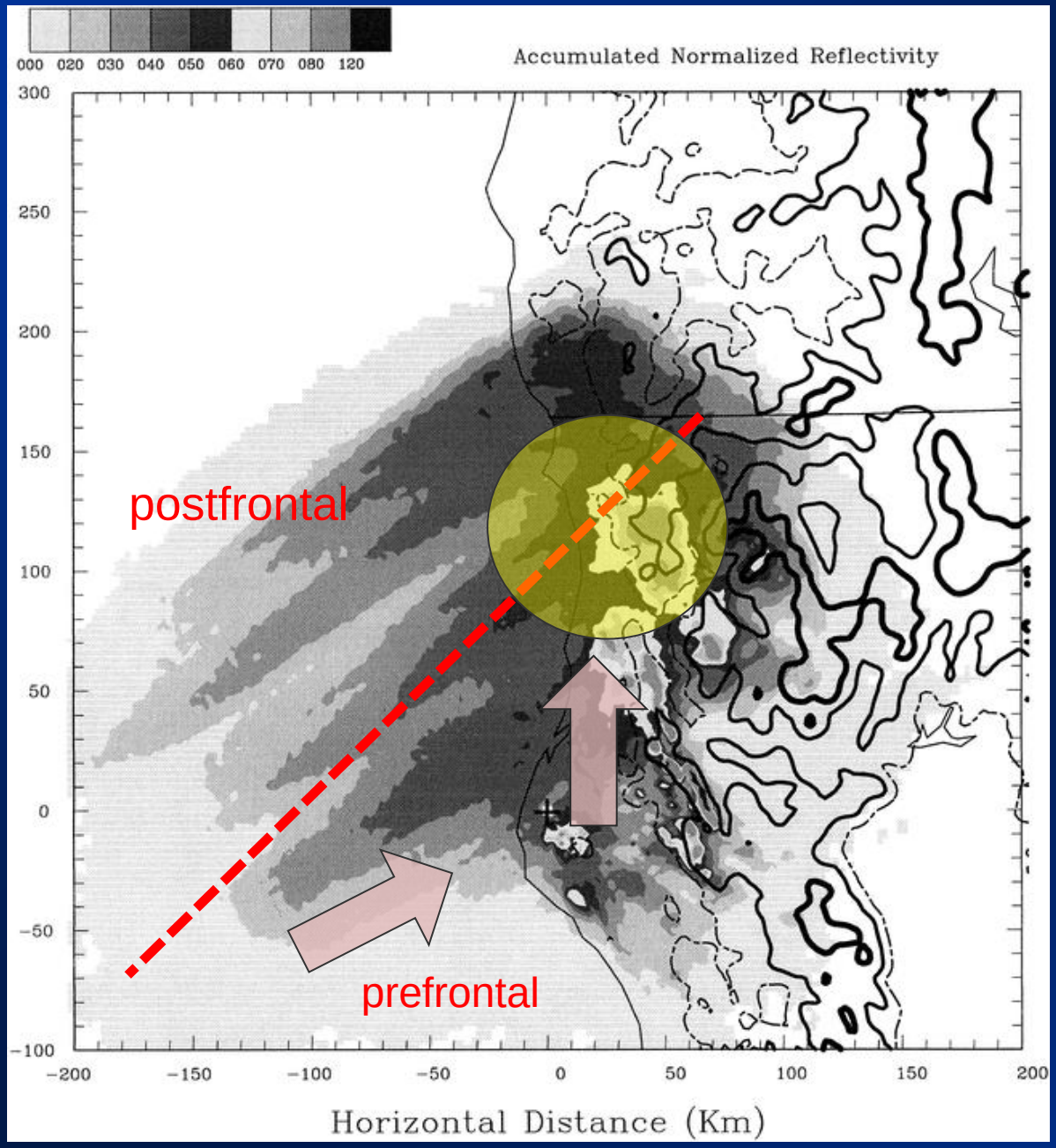

Yu and Smull (2000)

II: Convergence between the enhanced along-barrier flow and postfrontal flow

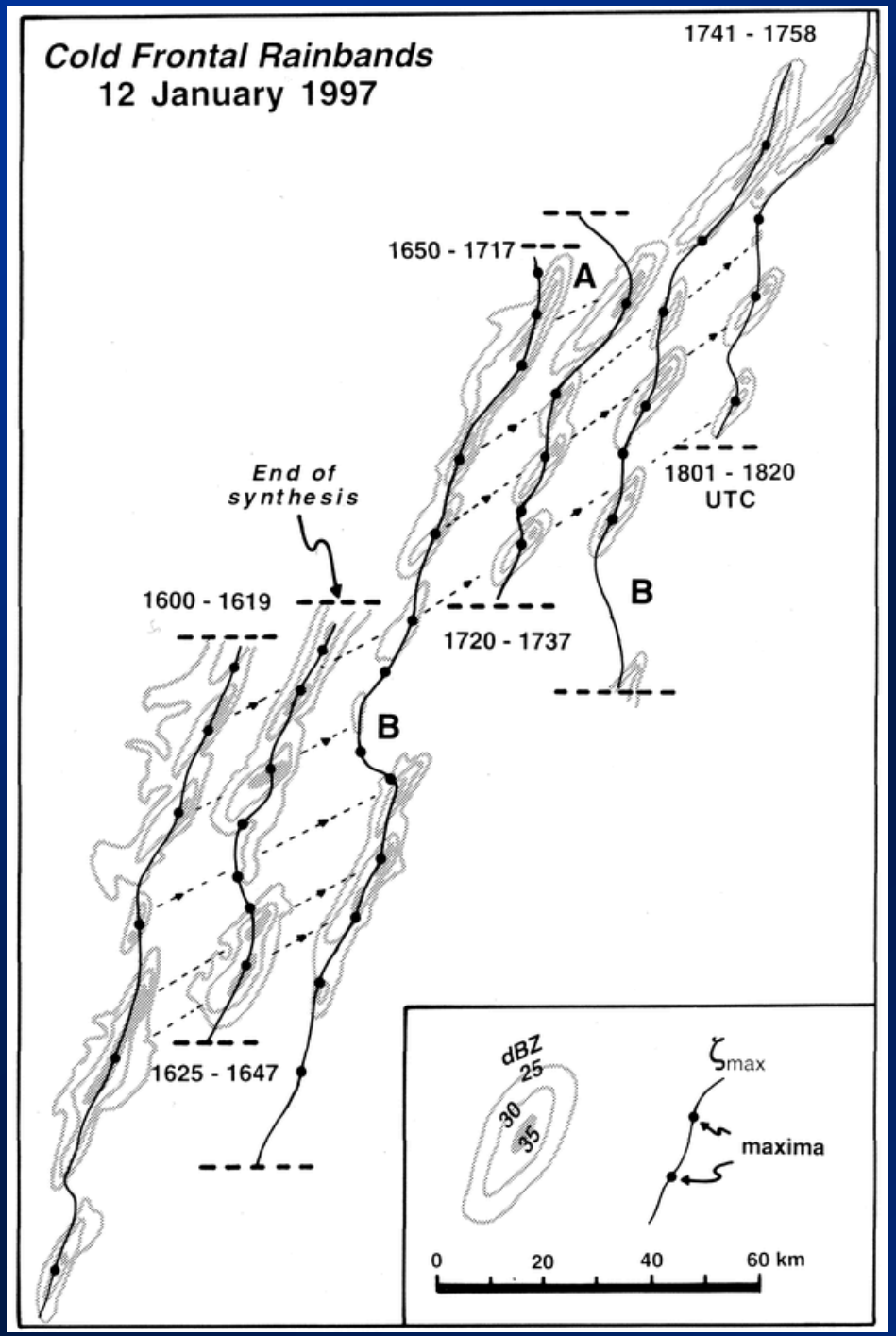

Wakimoto and Bosart (2000)

V: Distortion of the frontal zone

Yu and Bond (2002)

Before distortion

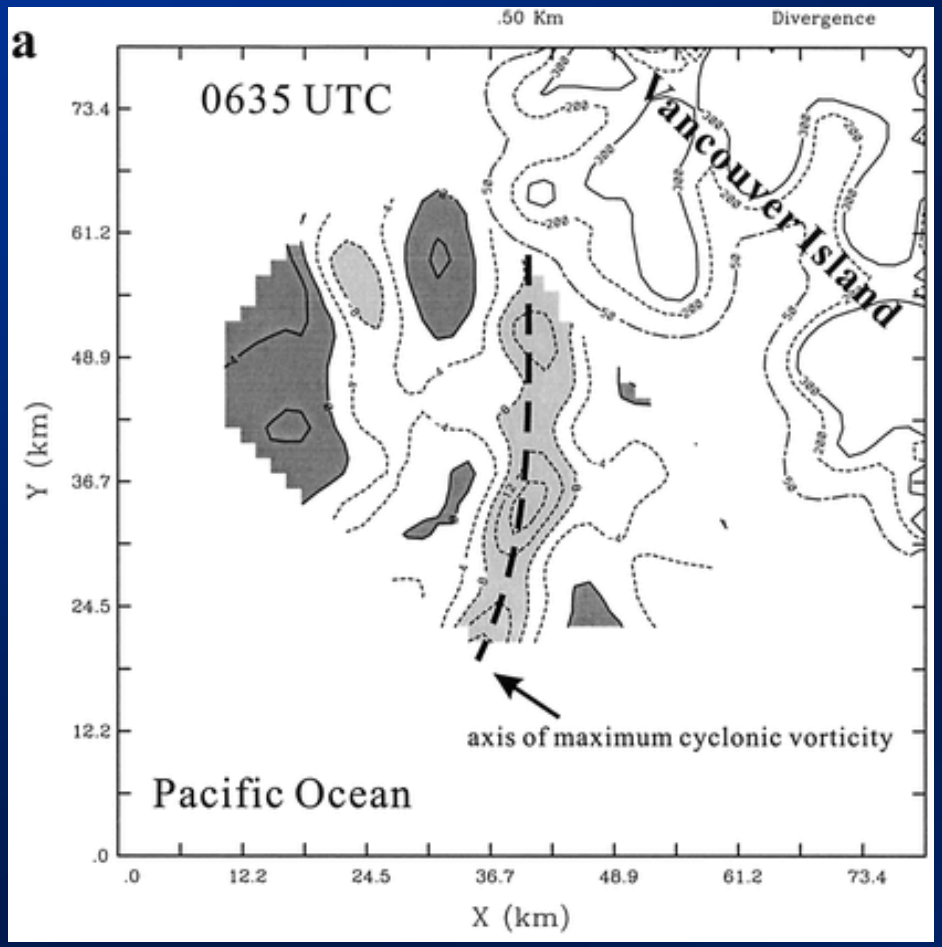

After distortion

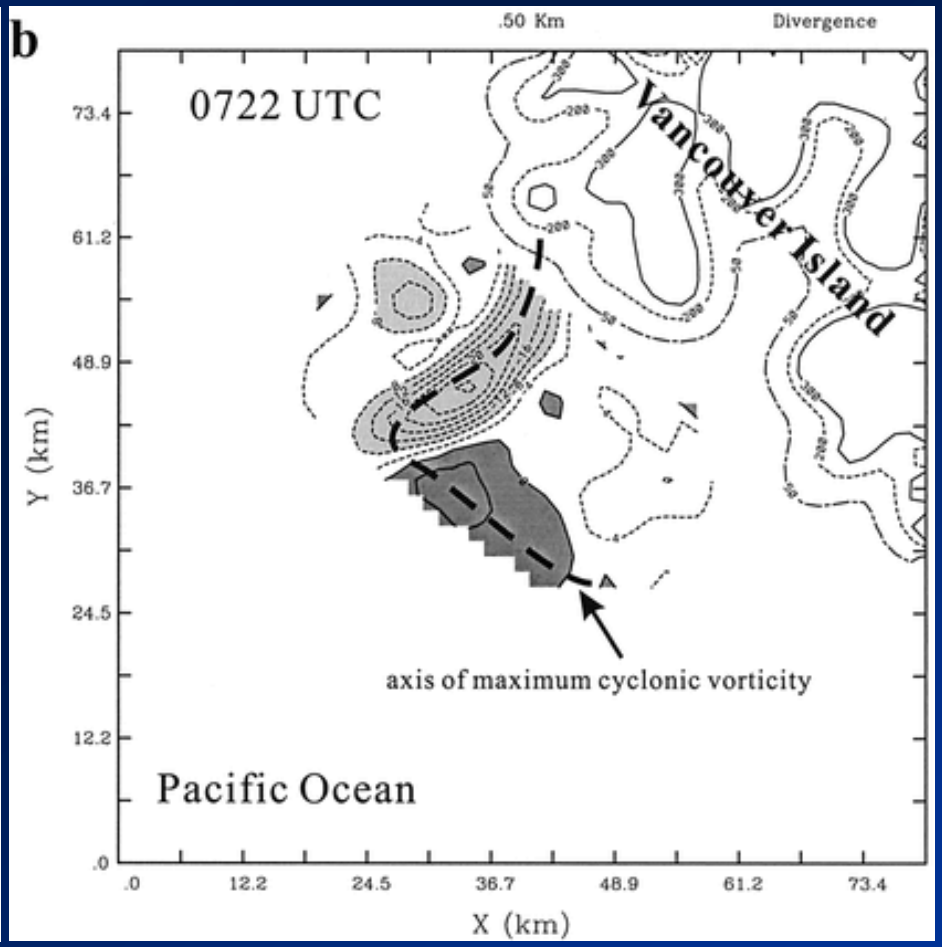

Trier et al. (1990)

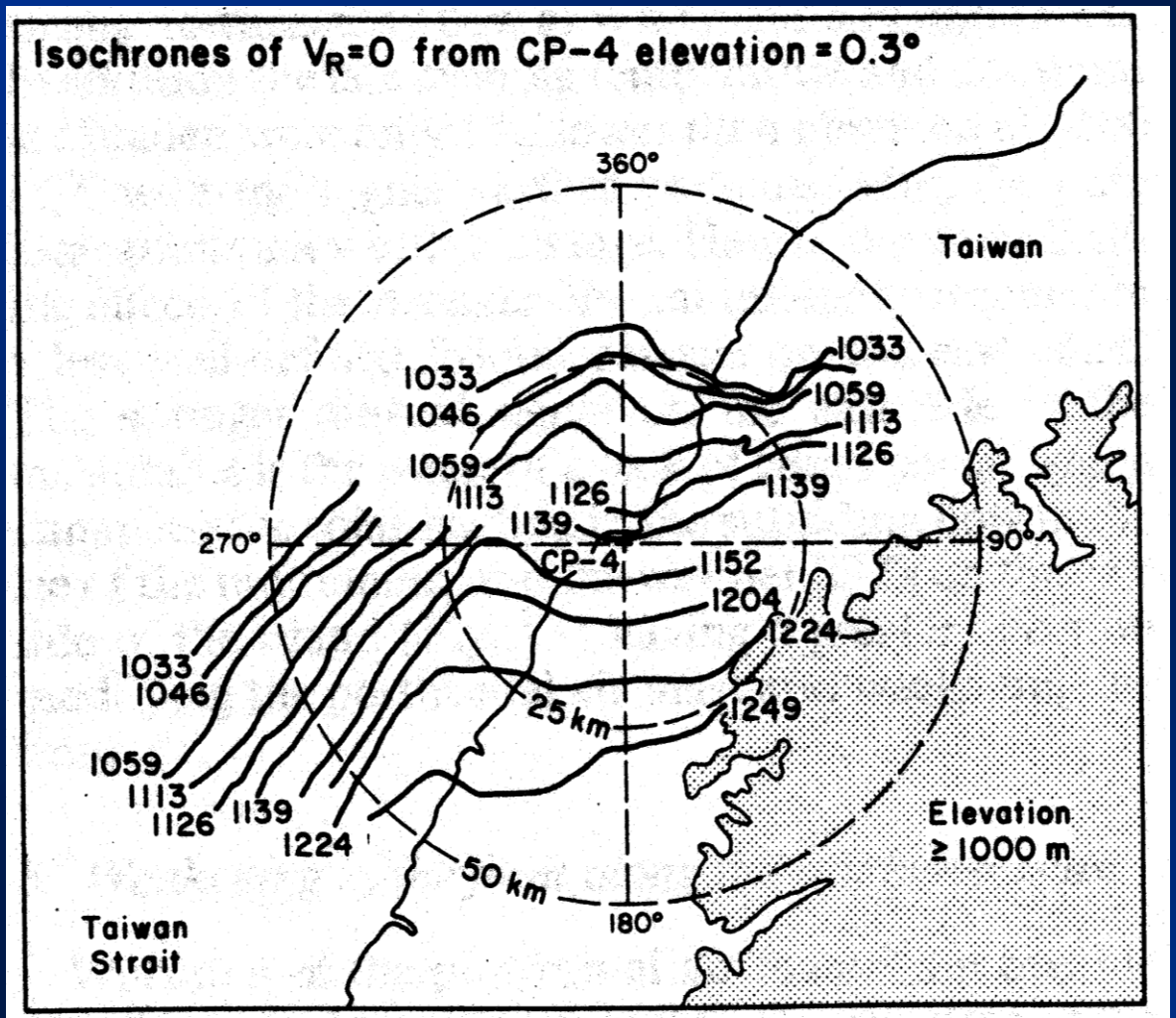

FIG. 18. Isochrones of the $V_R = 0$ m s^{-1} line from the 0.3° elevation PPI scan from the NCAR CP-4 Doppler radar depicting the horizontal wind shift associated with the cold frontal passage. All times on 8 June 1987 (LST). Shaded region corresponds to elevation in excess of 1000 m.

Trier et al. (1990)

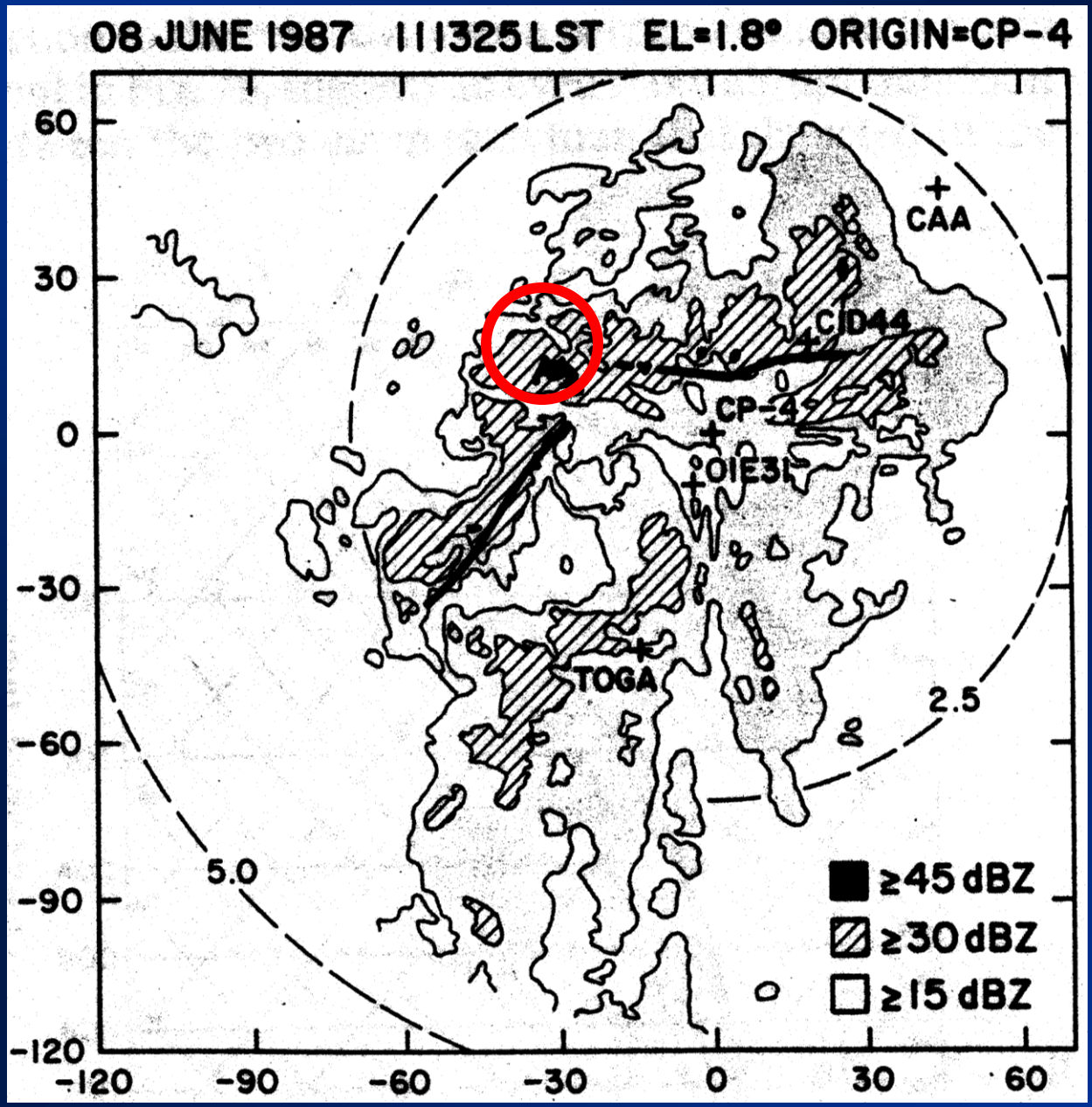

Strong interaction between the blocked, along-barrier flow and postfrontal flow (Neiman et al. 2004)

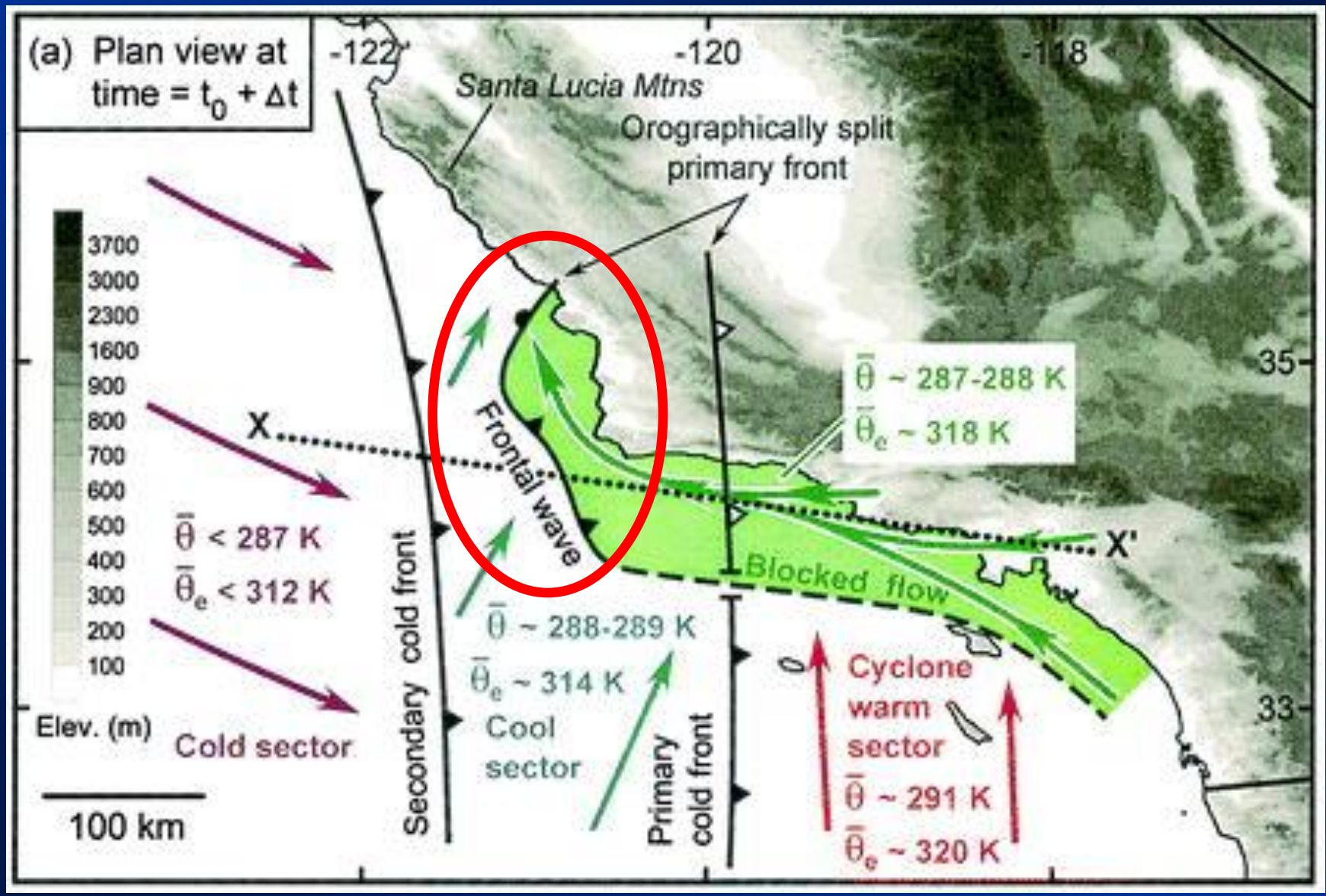

Neiman et al. (2004)